Curvature elasticity of smectic-*C* liquid crystals and formation of stripe domains along thickness gradients in menisci of free-standing films

N. V. Madhusudana *
Raman Research Institute, C V Raman Avenue, Bengaluru 560080, India

(Received 14 May 2020; accepted 25 August 2020; published 10 September 2020)

Smectic liquid crystals with a layering order of rodlike molecules can be drawn in the form of free standing films across holes. Extensive experimental studies have shown that smectic-*C* (Sm*C*) liquid crystals (LCs) with tilted molecules form periodic stripes in the thinner parts of the meniscus, which persist over a range of temperatures above the transition of the bulk medium to the Sm*A* phase in which the tilt angle is zero. The prevailing theoretical models cannot account for all the experimental observations. We propose a model in which we argue that the *negative curvature* of the surface of the meniscus results in an energy cost when the molecules tilt at the surface. The energy can be reduced by exploiting the allowed $(\nabla \cdot \mathbf{k})(\nabla \cdot \mathbf{c})$ deformation which couples the divergence of **k**, the unit vector along the layer normal, with that of **c**, the projection of the tilted molecular director on the layer plane. We propose a structure with periodic bending of layers with opposite curvatures, in which the **c**-vector field itself has a continuous deformation. Calculations based on the theoretical model can qualitatively account for all the experimental observations. It is suggested that detailed measurements on the stripes may be useful for getting good estimates of a few curvature elastic constants of Sm*C* LCs.

DOI: 10.1103/PhysRevE.102.032701

I. INTRODUCTION

Smectic liquid crystals (Sm LCs) are made of freely rotating rodlike molecules which are assembled in liquid layers. In the Sm*A* phase, the director (**n**), which is the average orientation direction of the long axes of the rods, is along the layer-normal direction (**k**), while in the Sm*C* phase **n** makes a tilt angle θ_t with **k** (Fig. 1) [1]. In view of the crystal-like elasticity of the Sm LC along **k**, it can be drawn in the form of free standing films (FSFs) across millimeter sized holes in glass plates [2]. The sample can be annealed so that the central part of FSFs has a flat structure with a well-defined number of layers, and investigations on such layers have led to various discoveries like that of hexatic phases, etc.

The flat central part is connected to the walls at the edge of the hole through a meniscus region in which the thickness increases continuously, mediated by edge dislocations in the layer structure. The dislocations are repelled by the large surface tension of smectic LCs ($\gamma \sim 0.02$ N/m) to the center of the meniscus (Fig. 2). Detailed experimental and theoretical studies [2] on Sm*A* menisci have shown that in the thinner parts close to the center, the dislocations have a Burgers vector equal to the layer spacing d. Closer to the wall, large Burgers vectors ($\geqslant$20 or so) mediate in the thicker parts, which gives rise to a two-dimensionally deformed structure made of parabolic focal conics. The meniscus surface has a circular shape, with a radius $R_M \geqslant 100\,\mu$m, except very close to the central flat region, in which it has an essentially linear slope [3]. By Laplace's law, the meniscus region will have a lower pressure $\Delta P = \gamma / R_M$ compared to the air pressure, the latter generating a compressive stress in the central flat layers.

If the FSF is made of a Sm*C* LC with tilted molecules, different features develop in the meniscus region. In addition to the two-dimensional (2D) pattern made of parabolic focal conics in the thicker parts, a radially oriented stripe domain (SD) pattern is observed in the thinner parts (for a recent review, see [4]). The spacing of the SD pattern decreases with the height h of the meniscus, and the pattern disappears below a critical thickness $\leqslant 1$ μm [3] before the meniscus region joins with the central flat part of the FSF. Periodic patterns often arise in Sm LCs to minimize the elastic energy when the layers cannot remain flat. For example, a thin Sm*A* sample taken on, say, a mica sheet treated to get a planar alignment of **n** with the top surface exposed to air is subjected to antagonistic boundary conditions. The sample exhibits a periodic focal conic structure [5]. A Sm*A* disc immersed in a nematic medium exhibits edge undulation arising from saddle-splay elasticity [6]. From the point of view of the problem discussed in this paper, an interesting case is a Sm sample taken in a wedge shaped cell with a small wedge angle. A periodic array of edge dislocations mediates the increase in the number of layers with the thickness of the sample, made visible under a polarizing microscope when the sample approaches the Sm*A*-Sm*C* transition point [7]. Flow fields can also drive undulation instabilities in smectics (for a recent example, see Ref. [8]), but our main interest in this paper will be equilibrium structures.

Over the past four decades, there have been numerous experimental studies and a few theoretical analyses of the SD patterns in the meniscus region of a Sm*C* FSF mentioned earlier. In the following we summarize the experimental studies, and outline the theoretical ideas put forward to elucidate the

*nvmadhu@rri.res.in

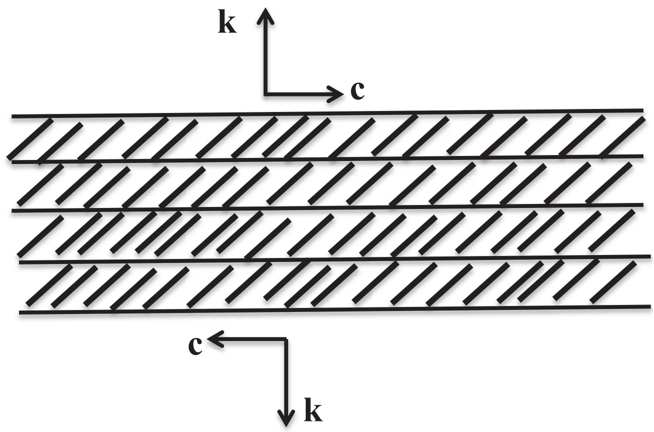

FIG. 1. Schematic diagram showing the layered structure of smectic-C liquid crystals. The director $\mathbf{n}$ is an apolar vector along the average orientation direction of the tilted rodlike molecules. Its projection on the layer plane is a polar vector $\mathbf{c}$, which is assumed to be a *unit* vector. $\mathbf{k}$ along the layer normal is also a *unit* vector. Note that the symmetry of SmC is preserved when *both* $\mathbf{k}$ and $\mathbf{c}$ change sign.

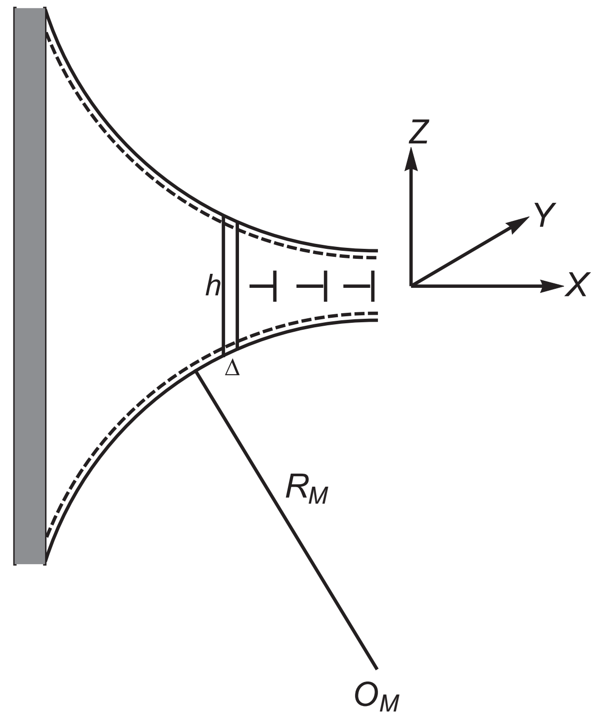

FIG. 2. Schematic diagram of the meniscus region of a free standing smectic film. Only the left section of a film taken between two parallel walls (shaded region) is shown. The thickness h of the meniscus decreases as one moves away from the wall along X, reaching a flat part with thickness h_F at $X = X_{\max}$. Edge dislocations located at the midplane of the meniscus mediate the variation in h. The Burgers vector of the dislocation (shown by the symbol **T** rotated by 90°) is equal to the layer thickness d near the thinner parts and several times d in the thicker parts. The surfaces of the meniscus have a circular shape with a radius $R_M \sim 100\,\mu$m. As the sample is cooled towards SmA to SmC transition temperature (T_{AC}), the director in the layers near the surface develops a tilt angle, and the corresponding $\mathbf{c}$ vector can be expected to develop a bend distortion by following the surface profile, shown by the dashed lines near the surfaces. It is argued in the text that this actually costs a positive energy, which is reduced by the formation of stripe distortions of the thinner parts of the structure with periodicity along Y. Δ is the small width of a slice with thickness h used in the theoretical analysis.

SD structures. Denoting the projection of the apolar $\mathbf{n}$ on the layer plane by the polar vector $\mathbf{c}$, Meyer and Pershan [9] noted that a splay deformation of the $\mathbf{c}$ field on the *surface* layer of a SmC sample can generate an electric polarization along $\mathbf{k}$, which can lower the energy of the sample. The surface can then be covered by SDs, each of which has a finite splay angle of $2\psi_0$ of $\mathbf{c}$ defining the domain, and separated by walls across which the $\mathbf{c}$ vector jumps by the same angle in the opposite sense. The walls penetrate a few layers of the sample, and energy considerations imply that at the lower surface the SDs are shifted by half their spacing in relation to those on the upper one. It is clear that this mechanism does not depend on the thickness (h) gradient of the meniscus region of a FSF. However, in all experimental studies, SDs have been found *only* in the meniscus region, and indeed are absent in any flat part in the meniscus which separates parts with h gradients [3].

In twist grain boundary (TGB) LCs blocks made of smectic layers consisting of a certain class of chiral molecules twist across grain boundaries with arrays of screw dislocations [1,2]. In a binary mixture exhibiting two TGB phases with upright (TGBA) and tilted molecules (UTGBC*, the asterisk signifying chiral twist) respectively, FSFs exhibited the SD structure in a thickness range in which the TGB LCs are untwisted [10,11]. Polarized fluorescence microscopy of the samples with added dye molecules clearly showed that in the SDs the layers themselves had periodic undulations [11].

When colloidal spherical particles are deposited in the central (flat) part of a FSF in a material exhibiting a lower temperature SmC*, the higher temperature SmA LCs developed meniscus regions around the particles, which were decorated by radial SDs [12]. A model interpreting the coronal SDs to be caused by the lower pressure (ΔP) in the meniscus, which gives rise to an undulation instability of the layers, has been proposed. Later similar studies [13] using both solid and fluid particle deposits clearly demonstrated that the coronal SDs persisted in SmA in a range of temperatures above the SmA-SmC (or SmC*) transition temperature (T_{AC}). In fact the main meniscus parts of the FSF close to the walls also exhibited the SDs in a similar range of temperatures. It has been experimentally established that in such materials, in the layers close to the *surface* of SmA FSFs, the director develops a tilt order which becomes stronger as T_{AC} is approached [14]. On the other hand, if the material has no underlying SmC phase, SDs do *not* develop either in the main meniscus region or around deposited particles on the FSF. This clearly demonstrates that the minimum requirement for the occurrence of SDs is a tilt order in at least the surface layers of FSFs. Thus the model developed in [12] for the coronal SDs is unlikely to be correct.

Optical observations on the SDs in the SmC phase have pointed to a structure in which there is a relative shift of half a period between the top and bottom surfaces of the meniscus [15], as was proposed in the early model of Ref. [9]. Atomic force microscopy (AFM) and phase shifting interferometry (PSI) of the SDs have clearly shown that the surface itself has a periodic height variation across the SD [3,16], which is of the order of a few percent of the spatial period w of the structure. w itself varies *linearly* with the local height h of the meniscus [3,4,15,16]. Loudet *et al.* [16] have developed a theoretical model of SDs, arguing that they arise due to an undulation instability of the layers when the sample is cooled below T_{AC}. In this model, it is assumed that the layers are strongly anchored at the walls, and that the reduction in the layer spacing due to the tilting of **n** with respect to **k** leads to a dilative stress on the Sm*C* layers in the meniscus region, which is relieved by undulations. The surfaces of the FSF also undulates and the surface tension γ also contributes to the free energy, which is taken to be that of the Sm*A* phase under a dilative stress [16]. Numerical results show that the period $w = 0.85\,\mu$m for a sample thickness $h = 10\,\mu$m, and further, $w \propto \sqrt{h}$. On the other hand, the experimental results show that $w \approx h$, and $w \propto h$ [3,4,15,16]. Further, the undulation instability [1,2] found in smectics subjected to a dilative strain is a metastable structure, which is replaced by edge dislocations that move in to fill space. On the other hand, the SDs in Sm*C* LCs have been observed to be stable over days [3,15], even though the meniscus region easily accommodates edge dislocations. Even in compounds which exhibit the Sm*A*-Sm*C* sequence, the SD patterns are absent in intermediate flat regions of the meniscus, though they are seen in neighboring parts of the meniscus with thickness gradients [3]. Further, when the area of a thick Sm*C* FSF is suddenly increased, holes with reduced number of layers, and thickness gradients sporting radial SD patterns around their periphery, are generated [17]. Once again the flat regions on either side of the periphery of the expanding holes are devoid of SD patterns. Thus, *thickness gradients* are essential for the formation of SD patterns. Further, SDs have been found in a material which undergoes a first order transition directly from the nematic (*N*) to Sm*C* phase, in which the layers are not subjected to the dilative strain due to thermal variation of the layer spacing d [18]. More interestingly, in a compound with a transition from the Sm*C* in which the tilt angles of **n** in successive layers are synclinic (SmC_S) to one in which they are anticlinic (SmC_A), the SDs which formed in the SmC_S LC *disappear* on transition to the SmC_A LC [18]. The observation brings out the importance of the synclinic tilting of **n** to be the real cause of SDs, and not the dilative strain caused by the tilting. However, another system with a direct *N*-Sm*C* transition exhibits the SD pattern in the Sm*C* meniscus, but the PSI scan shows hardly noticeable surface undulations, with an amplitude <10 nm [19]. The above summary of the present state of research on SDs exhibited by FSFs clearly brings out the crucial role of the tilting of **n**, even if only in the layers near surfaces. The prevailing theoretical models [9,16] are clearly inadequate to account for the observations. In the following section we argue that a detailed analysis which takes into account a few different terms necessary to describe the curvature elasticity of SmC_S LCs [1] is needed to understand the formation of SDs.

II. THEORETICAL MODEL

Sm*A* LCs are characterized by a relatively simple elastic response. Any gradients in layer spacing d cost a large energy, and the only *curvature* distortion corresponds to that of the bending of layers or, equivalently, the splay distortion of **n**, which costs a very low energy. Sm*C* LCs are characterized by the additional vector **c**, which can have the usual splay, twist, and bend curvature distortions of any vector field. In addition, the layer bendings can also couple with the **c**-vector fields requiring several elastic constants to describe the possible curvature distortions of the medium. A few different approaches have been proposed for describing the distortions, and a comprehensive summary of the models has been given by Stewart [20]. In the following we find it convenient to use the description based on **c** and **k** vector fields. Both **c** and **k** are *unit* vectors, and with reference to Fig. 1, and the usual understanding that the tilt angle θ_t between **n** and **k** is acute, **c** points along the projection of **n** on the layer plane. If the sign of **k** is reversed, that of **c** is reversed as well, and only those curvature distortions in which the **c**- and **k**-dependent terms totally add up to an even number are allowed.

Typically, the Sm*C* stripes of a given periodicity form a *closed* chain without coming into contact with any solid boundaries, in the meniscus region around the central flat film. Similarly, the coronal stripes around a deposited particle on the central part of the FSF also form a closed chain. This allows us to simplify the problem, and assume the FSF of Sm*A* LC to be formed between two *parallel* vertical walls (Fig. 2) with edges lying in the *YZ* plane, and *extended* along the *Y* axis, so that the equilibrium SD structure can be found by minimizing the energy *density*. Both the top and bottom surfaces of the meniscus have a circular shape in the *XZ* plane, with a radius R_M, except very close to the boundary with the central film of uniform thickness. The surface layers with **k** pointed towards the center of the circle develop a tilt angle even a few degrees above T_{AC}. We first consider the temperature of the sample to be below T_{AC}, so that it is in the Sm*C* phase. Let us assume that the **c** vector in the surface layer naturally follows the curved profile, and develops a nonzero bend distortion vector $\mathbf{c} \times \mathbf{curl c}$ with a magnitude c^2/R_M, and oriented along $-\mathbf{k}$. The bend vector itself has a splay distortion as it is aligned with **k**. This of course would lead to a crowding of the ends of the tilted molecules at the surface, which is not favored. In analogy with the saddle-splay elasticity in nematics, we introduce the elastic term $k_{SS}\,\nabla \cdot (\mathbf{c}\nabla \cdot \mathbf{c} + \mathbf{c} \times \nabla \times \mathbf{c})$ which is of course a surface term. The above argument shows that k_{SS} is negative, resulting in a *positive* energy density in the medium. Considering a thin vertical slice of width Δ, across which the meniscus height h can be assumed to be constant (Fig. 2), the average energy *density* of the slice due to the above term is given by

$$F_{SS} = -2k_{SS}/(hR_M). \tag{1}$$

The factor 2 in the above arises as there are two equivalent surfaces in the meniscus. A surface **c** field which is perpendicular to the plane of the paper in Fig. 2 does not necessarily reduce the energy density, as the ends of the *tilted* molecules are still crowded at the surface, costing energy. Introducing the vector $\mathbf{b} = \mathbf{k} \times \mathbf{c}$, it is clear that $\mathbf{b}$ will have the bend distortion in the latter case. We assume that k_{SS} introduced above adequately captures the physical process, and ignore $\mathbf{b}$-dependent terms in the following. We can note that around layer steps in the FSF the $\mathbf{c}$ vector aligns parallel to the step edge, i.e., the dislocation [3,17]. However, in the meniscus the edge dislocation is located at the center, in which the $\mathbf{c}$ vector has been found to have the orthogonal orientation, as shown in Fig. 1(a) of Ref. [7]. Recently cryotransmission electron microscopy has been used to image the edge dislocations of a thin (∼100 nm) SmC^* sample in bookshelf geometry [21]. If the tilt plane is *orthogonal* to the dislocation, the core region is found to be small (∼layer spacing). On the other hand, if the dislocation is in the tilt plane, the core is spread over a few layers in a direction along layer normal (Fig. 4 in Ref. [21]), which probably costs a higher energy. We assume that the tilt plane is orthogonal to the dislocation line, which simplifies the analysis.

The structure of the meniscus can change to lower the positive energy given by Eq. (1) due to the negative curvature of the surface, by exploiting other curvature elasticities of the medium. As k_{KC} $(\nabla \cdot \mathbf{k})(\nabla \cdot \mathbf{c})$ is an allowed deformation [20] which can cost a negative energy, we propose a structure in which the meniscus height h is constant. The layers are assumed to bend in the YZ plane, periodic along Y as shown in Fig. 3. Again considering a slice of width Δ along the X axis, in which the height of the meniscus is h, all the layers are assumed to bend in circular arcs with an angular spread α, centered on some line parallel to the X axis and lying *below* the lower surface, to form a V-shaped section. The two neighbors of this section will have an inverted V shape, with the layers bending about centers lying *above* the top surface, such that there is a smooth continuity of all the layers across the sections. The circular shape of the bent layers ensures that the layer spacing does not have any gradient, thus avoiding a costly elastic energy, and only the weak elasticity of curvature deformations contribute to the energy of the structure. Further, as the height h does not change on the formation of the periodic structure, there is no net change in the surface area, i.e., there is *no additional cost due to surface tension*. Thus if b is the *width* along the Y axis of the slice before bending of the layers, the total area of the two surfaces exposed to air is $2b\Delta$. If R_i is the radius of the lower surface, that of the upper surface is given by $R_u = R_i + h$. As the volume of the slice is preserved after bending, α, the angle of bending [Fig. 3(a)] satisfies $\alpha h(2R_i + h)/2 = hb$. This value of α also ensures that the total area exposed to air after bending, viz., $\alpha(2R_i + h)\Delta$ is also unaltered, as mentioned above. The width of the curved central layer at $h/2$ is given by $\alpha(R_i + h/2)$ which is equal to that of the section before the bending of the layers, viz., b. This means that the length of the edge dislocation line, which resides at the center of the meniscus, remains unaltered after the change in structure, and we can assume the dislocation energy to be unaffected by the change, to a good approximation. We ignore the presence of the dislocations in further analysis of the problem, but come back to point out their possible influence towards the end of the paper.

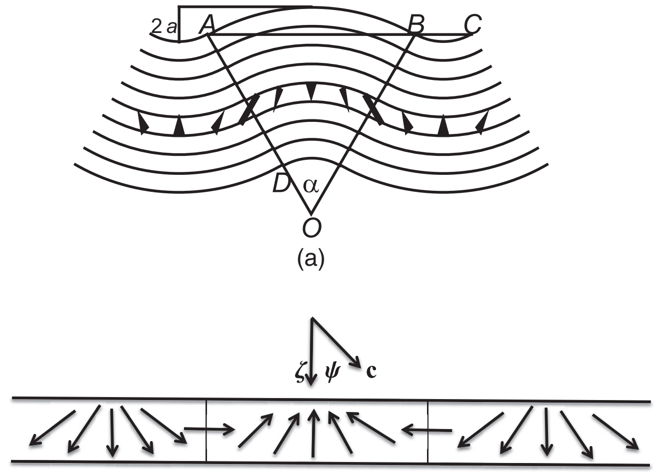

FIG. 3. (a) Schematic diagram of the proposed model of the stripe domains in the thinner regions of the meniscus of a free standing film of SmC liquid crystal. Side view along X of a slice as shown in Fig. 2, which is also along the ζ axis of the *local* cylindrical coordinate system, and pointed into the plane of the diagram. In the central V-shaped section, the layers bend in circular arcs of angular extent α around the center at O. The layers in the neighboring sections bend around symmetrically located centers above the uppermost layer, producing inverted V-shaped sections. The spatial distortion of the tilted director $\mathbf{n}$ field is shown in a middle layer. The thicker ends of the triangular symbols signify projections towards the reader. Both the layers and the $\mathbf{n}$ fields vary smoothly across the neighboring sections. The radius of the nearest layer from O is R_i = OD, and that of the upper-most layer OA $= R_i + h$. The spatial period of the stripe pattern is w = AB + BC, and the amplitude of the surface modulation is given by a. (b) Top view showing the $\mathbf{c}$-vector field of the stripe domains in a slice of width Δ. Note that both the $\mathbf{c}$ field and the corresponding $\mathbf{k}$ field as seen in (a) have opposite divergences in neighboring sections.

We introduce a *local* cylindrical coordinate system $\mathbf{r}\boldsymbol{\phi}\boldsymbol{\zeta}$ with the origin at O and the $\boldsymbol{\zeta}$ axis along the X axis of the Cartesian system introduced earlier, $\mathbf{r}$ along the radius vector, and with the azimuthal coordinate angle ϕ measured from the vertical radius vector bisecting the V-shaped section (Fig. 3). We assume that Δ is so small that all gradients along ζ can be set equal to 0 within the sliced section. $\mathbf{k}$ is the unit vector along $\mathbf{r}$, and we can note that the layer saddle splay term $\boldsymbol{\nabla} \cdot (\mathbf{k}\, \boldsymbol{\nabla} \cdot \mathbf{k})$ vanishes in the proposed structure, and there is no energy gain in the SmA phase. It means that the only reason for the layer bending with nonzero $\boldsymbol{\nabla} \cdot \mathbf{k}$ is the coupling with $\boldsymbol{\nabla} \cdot \mathbf{c}$ which is possible only in the SmC phase.

If the elastic constant k_{KC} introduced above has a positive value, the sign of $\boldsymbol{\nabla} \cdot \mathbf{c}$ will be negative to lower the energy of the structure [Fig. 3(a)]. If $\psi(\phi)$ is the azimuthal angle made by $\mathbf{c}$ with the (local) $\boldsymbol{\zeta}$ axis [Fig. 3(b)], we assume that ψ varies from $+\pi/2$ to $+3\pi/2$ as ϕ varies from $-\alpha/2$ to $\alpha/2$ across the section. By definition $c_r = 0$, and the other components are $c_\phi = \sin\psi$, and $c_\zeta = \cos\psi$. The assumed range of $\psi(\phi)$ ensures that both $\mathbf{k}$ and $\mathbf{c}$ vectors vary smoothly across neighboring sections without any walls with discontinuities in the vector fields.

The curvature distortions are given by

$$\nabla \cdot \boldsymbol{k} = \frac{1}{r};\ \nabla \cdot \boldsymbol{c} = \frac{\cos\psi}{r}\frac{\partial\psi(\phi)}{\partial\phi};$$
$$\boldsymbol{c} \times \nabla \times \boldsymbol{c} = \left(\frac{(\sin\psi)^2}{r}, -\frac{\sin\psi\cos\psi}{\boldsymbol{r}}\frac{\boldsymbol{\partial}\psi(\phi)}{\boldsymbol{\partial}\phi}, \frac{(\sin\psi)^2}{r}\frac{\boldsymbol{\partial}\psi(\phi)}{\boldsymbol{\partial}\phi}\right). \quad (2)$$

The elastic energy density of the structure has many contributions. The cost of bending the layers is given by

$$F_B = \frac{k_B}{2}(\nabla \cdot \boldsymbol{k})^2 = \frac{k_B}{2r^2}. \quad (3)$$

Assuming the one constant approximation for both the splay and bend distortions of the **c** field, the relevant energy density is given by

$$F_C = \frac{k_C}{2}\left[(\nabla \cdot \boldsymbol{c})^2 + (\boldsymbol{c} \times \nabla \times \boldsymbol{c})^2\right] = \frac{k_C}{2r^2}\left[(\sin\psi)^4 + \left(\frac{\boldsymbol{\partial}\psi(\phi)}{\boldsymbol{\partial}\phi}\right)^2\right]. \quad (4)$$

The coupling between the splay deformations of both **k** and **c** mentioned earlier leads to the energy density

$$F_{KC} = k_{KC}\ (\nabla \cdot \boldsymbol{k})(\nabla \cdot \boldsymbol{c}) = k_{KC}\frac{\cos\psi}{r^2}\frac{\partial\psi(\phi)}{\partial\phi}. \quad (5)$$

The saddle-splay-like term of **c** deformation mentioned at the outset cancels out in the proposed structure:

$$F_{SS} = k_{SS}\nabla \cdot (\boldsymbol{c}\ \nabla \cdot \boldsymbol{c} + \boldsymbol{c} \times \nabla \times \boldsymbol{c}) = 0. \quad (6)$$

Another total divergence term which depends on both **k** and **c** is

$$F_{\mathrm{SKC}} = k_{\mathrm{SKC}}\ \nabla \cdot (\boldsymbol{k}\ \nabla \cdot \boldsymbol{c} + \boldsymbol{k} \times \nabla \times \boldsymbol{c}). \quad (7)$$

It is interesting to note that the $\nabla \cdot (\mathbf{k}\,\nabla \cdot \mathbf{c})$ part of the above equation is essentially the surface term introduced in Ref. [9], but it has a null value in the structure proposed by us. [It can be pointed out that this term is different from the k_{KC} term of Eq. (5)]. $\mathbf{k} \times \nabla \times \mathbf{c}$ has only a nonzero ϕ component, and as the structure is assumed to extend along the Y axis, the surface contribution arising from this term can be ignored. The spatial dependence of **c**, or equivalently $\psi(\phi)$, can be obtained by minimizing the total energy density. Only F_c given by Eq. (4) has a quadratic dependence on the gradient term, and the Euler-Lagrange equation leads to the following relation:

$$\int_0^{\alpha/2} d\varphi = \frac{\alpha}{2} = \int_\pi^{3\pi/2} \frac{d\psi}{\sqrt{A + (\sin\psi)^4}}, \quad (8)$$

where we have used the symmetry of the structure in the given section, and A is a constant of integration.

The total elastic energy density as a function of the location in the section is given by

$$F_T = F_B + F_C + F_{KC}. \quad (9)$$

The energy density *averaged* over the volume of the section is given by

$$F_S = \frac{4}{\alpha\ h(2R_i + h)}\int_{R_i}^{R_i+h} dr \int_0^{\frac{\alpha}{2}} F_T r d\varphi = \frac{4\ \mathrm{Ln}\left(\frac{R_i+h}{R_i}\right)}{\alpha\ h(2R_i + h)}\left\{\frac{1}{4}k_B\alpha - k_{KC} + \frac{1}{2}k_C\int_\pi^{3\pi/2}\frac{\left(A + 2(\sin\psi)^4\right)}{\sqrt{A + (\sin\psi)^4}}d\psi\right\}. \quad (10)$$

In the above, the volume of the V-shaped section is $0.5\alpha h(2R_i + h)\Delta$. As we should compare the energy density of the periodic structure of the meniscus with that without it as given by Eq. (1), we should also take into account the *changed* contribution from the bend of **c** vector as it follows the circular surface of the meniscus. Experimental studies [3,16] as well as the results of calculations based on the model to be presented below show that the amplitudes of the periodic surface distortions are quite small. We can estimate the reduced contribution to be given by

$$F_M = -2k_{SS}\langle\cos^2\psi\rangle/(hR_{\mathrm{M}}), \quad (11)$$

in which the average of $\cos^2\psi$ is calculated over the angular width α of the section. The total averaged energy density of the periodically distorted structure is

$$F_{TS} = F_S + F_M. \quad (12)$$

Two lengths which have been measured in relation to the height h are as follows:

(i) the width w of the stripe which is given by $AC = AB + BC$ in Fig. 3(a),

$$w = 2(2R_i + h)\sin\alpha/2; \quad (13)$$

(ii) the amplitude a of the layer displacement is given by half the height difference between the crest of a given section and the trough of its neighboring section [Fig. 3(a)],

$$a = (R_i + h/2)(1 - \cos\alpha/2). \quad (14)$$

The curvature elastic constants pertaining to distortions in the **c** field, viz., k_{SS}, k_C, and k_{KC}, depend on the tilt order parameter, and while k_{KC} and k_{SS} can be expected to be proportional to the tilt angle θ_t, $k_C \propto {\theta_t}^2$ [20]. We have made calculations using the following set of parameters: $R_M = 200\,\mu$m, $k_B = 20 \times 10^{-12}$ N, $k_C = 3 \times 10^{-12}$ N, $k_{SS} = -9 \times 10^{-12}$ N, and $k_{KC} = 12 \times 10^{-12}$ N. The two parameters defining the structure at any given height h are R_i and α. For example, when $h = 5\,\mu$m, in the absence of the stripes, the energy given by Eq. (1) is $F_{SS} = 0.018\ \mathrm{J/m^3}$. At any given R_i, the average energy density of the stripe structure F_{TS} exhibits a minimum as a function of α. The minimized value, which remains positive, decreases as R_i decreases. For $R_i \sim$ a few layer spacings (d), the spatial deformations in **k** and **c** fields become very strong in the layers close to O, and can be thought of as forming the core of the partial disclinations in the two fields. The core region loses the layering and the orientational orders, and the transformation of course costs a relevant energy. The total energy of the structure should again start to increase as R_i is reduced below a few times d. We assume that the minimum occurs at $R_i = 10$ nm. The minimum energy of $0.0098\ \mathrm{J/m^3}$

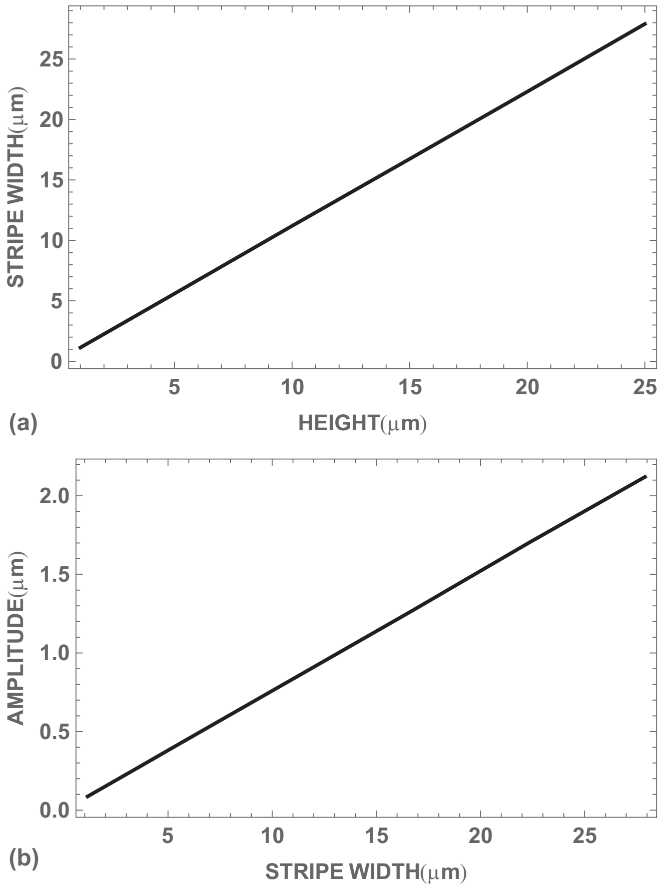

FIG. 4. (a) Variation of the stripe width w with the height h of the meniscus in the SmC phase. The linear dependence is in accord with experimental results [3,16]. (b) Variation of the amplitude a of the periodic surface profile of the stripes, as a function of the stripe width w. The relative magnitude of a is a few times larger than the experimental value, but the linear dependence reflects the experimental trend [3,16].

occurs for $\alpha = 1.18$ radians. As this energy is smaller than that for the meniscus without the stripes, the stripe structure is favored. Similar calculations at other values of the height h lead to similar results. Remarkably, the minima occur for $\alpha = 1.18$ radians independent of the height. This in turn leads to the result that the stripe width w defined in Eq. (13) varies essentially *linearly* with h, and for the parameters chosen, $w \approx h$ [Fig. 4(a)]. The linear dependence has been noted in some experiments [3,16]. The amplitude of the periodic surface height variations defined in Eq. (14) in turn varies linearly with w [Fig. 4(b)], and is ~6 or 7% of w, reflecting the experimental trend [3,16], though the measured value of a/w is only ~1%.

Though the energy of the stripe domain is lower than that of the meniscus without stripes, its sign remains *positive*. This means that the stripes do not form in the central part of a FSF with *flat* layers, in which the **c**-vector field can be assumed to be undistorted. We may also note the following points in relation to some experimental results: (i) The positive energy of the undistorted meniscus given by Eq. (1) has its origin in the *negative curvature* of the meniscus. In fact the actual curvature of the meniscus $(1/R_M)$ is unimportant, as long as the curvature is large enough to cost a sufficiently high positive energy given by Eq. (1). The parameters of the SD pattern (w and a) depend mainly on k_B, k_C, and k_{KC} and *not* strongly on k_{SS}. Indeed the part of the meniscus close to the central flat film has a negligible curvature [3] and hence also the associated positive energy. As a result, the SD structure forms above a threshold value of the thickness h [3]. (ii) In some samples cooled rapidly, the second neighbor SD stripes at the thinnest part bend around and join to loop around a central stripe [3]. From Fig. 3(a), it is clear that the outer stripes with inverted V sections can rotate around the central vertical axis passing through O, to smoothly join with each other, as they are geometrically compatible. This structure probably has a higher energy than the one which just ends at a critical meniscus thickness mentioned above, and has not been seen in the systems reported in Ref. [4]. (iii) The plot of a vs w reported in Ref. [3], which has a compressed scale along the horizontal axis compared to the vertical one, has a more rounded crest compared to the sharper trough, which is compatible with the structure shown in Fig. 3(a). (iv) The experimental amplitude of surface undulation is ~1% of the stripe width [3,16], while the calculated one is several times larger. From Eqs. (13) and (14),

$$\frac{a}{w} = \frac{1}{4}\tan\frac{\alpha}{4}. \tag{15}$$

The ratio which depends only on the angle α, reduces with the angle. Again, with $R_M = 200\,\mu$m, if the elastic constants are $k_B = 19.5 \times 10^{-12}$ N, $k_C = 1\,10^{-12}$ N, $k_{SS} = -9 \times 10^{-12}$ N, and $k_{KC} = 7 \times 10^{-12}$ N, α is reduced to 0.7 rad, and $a/w = 0.044$. But as α is lowered, the ratio of stripe width to the sample thickness *w/h* is also reduced to ~0.7, whereas experimentally, the latter ratio is ~1. We will comment later on a possible origin of the low value of observed *a/w,* especially in the case reported in Ref. [19], in which it is ~0.001. (v) In an experiment involving a sudden increase in the area of a *thick* FSF [17], the holes generated also develop a thickness gradient at their peripheries, in which radial SD patterns are formed beyond a critical thickness. As the holes expand, the peripheral region gets stretched, but the number of SD stripes does not vary significantly. From Fig. 3, a change in the number of stripes would require a major structural rearrangement of the bent layers, which is a slow process.

As the sample is heated above the SmC to SmA transition temperature T_{AC}, the tilt order is lost in the bulk, i.e., in the interior layers of the FSF. However, the tilt order persists near the surfaces [14], decreasing in strength as the temperature is increased. We make the simplifying assumption that a relatively small and uniform tilt order persists over some thickness δ near the surfaces of the sample, and the order vanishes in the rest of the sample (Fig. 5).

It is clear that, unlike in the SmC phase, the elastic terms favoring the formation of stripes which require the **c**-vector field are effective only in the two surface regions, whose relative contribution decreases as the thickness of the meniscus h increases. Consequently, in the free energy density averaged over the volume of a V-shaped section, while the k_B term is multiplied by $\mathrm{Ln}((R_i + h)/R_i)$ as in Eq. (10), the k_{KC} and k_C terms are multiplied by $\mathrm{Ln}[(R_i + h)(R_i + \delta)/R_i(R_i + h - \delta)]$, reflecting the reduced

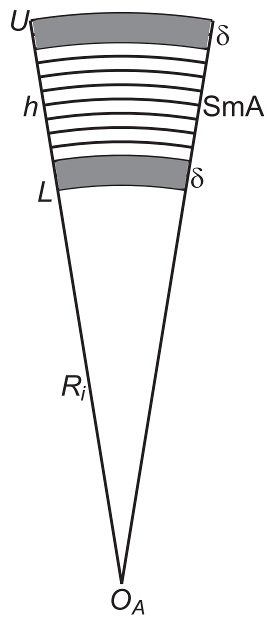

FIG. 5. Schematic diagram of a section of stripe above the Sm*C* to Sm*A* transition temperature T_{AC}. The shaded areas of thickness δ at the top and bottom surfaces are assumed to have a nonzero tilt order, while the rest of the medium is in the Sm*A* phase without any tilt order. As described in the text, in order to reduce the positive elastic energy of bending of the layers, the center O_A is pushed far away from the surface, increasing $R_i(=O_AL)$ to tens of micrometers.

contributions from the latter terms. As the temperature is increased just above T_{AC}, we expect the stripe domain in the meniscus with the largest value of h, which occurs just adjacent to the two-dimensional structure made of parabolic focal conics, to become unstable as its energy increases. The tilt order in the surface layers can be expected to be lower than in the Sm*C* phase, and we use the following parameters in the calculations: $R_M = 200\,\mu$m, $k_B = 10\times10^{-12}$ N, $k_{SS} = -3\times10^{-12}$ N, $k_C = 0.6\times10^{-12}$ N, $k_{KC} = 4\times10^{-12}$ N, and $\delta = 20$ nm. Assuming that the stripe domain emerges from the two-dimensional structure at $h = 25\,\mu$m, the energy density in the absence of the stripes, arising from the k_{SS} contribution [Eq. (1)] is 0.0012 J/m^3. The dominant layer bending contribution can be reduced by increasing R_i (Fig. 5). As the stripe structure is found to smoothly emerge from the focal conic structure, with the periodicities in the two being comparable [15], the angle α has to be reduced as R_i is increased (Fig. 5). The average energy density decreases as R_i is increased, the rate of change decreasing as well. When $R_i = 80\,\mu$m, and $\alpha = 0.18$ rad, the energy density is just lower than that of the meniscus without the stripe. This can be considered as the threshold condition for a stable stripe structure. For a smooth structure in the meniscus, as in the Sm*C* phase, we can assume that R_i and α remain independent of h. As R_i is much larger than h, it is clear from Eq. (13) that the stripe width w is not very sensitive to h, unlike in the Sm*C* phase. For the parameters given above, w is about 30 μm, and reduces by about 10% as h is decreased from 25 to 5 μm. Indeed, experimentally the stripes have been found to become straight [13], without the branching needed to accommodate the decrease in w with that in h as found in the Sm*C* phase. The amplitude a [Eq. (14)] is also essentially independent of h, and is found to be ~1% of w, much less than in the Sm*C* phase. Indeed, the energy density slowly decreases as R_i is increased further. As both R_i and α have to change over the entire meniscus region, and the relevant viscosities of the Sm*A* phase are quite large, the process is quite sluggish at low temperatures, and the stripes have been found to be fairly long lived. However, as the temperature is raised, the viscosities and the tilt order at the surface decrease, and the process mentioned above accelerates: R_i can be expected to increase with time, inevitably reducing the amplitude a of the structure, which can be expected to *fade away* with time, as found in experiments [13,4]. When the sample is cooled from a high temperature in the Sm*A* phase, the stripes are not expected to form until T_{AC} is approached. Indeed experimentally, very fine stripes have been found to form near the edge of the focal conic domains close to T_{AC}, and then pervade the meniscus as the temperature is lowered across T_{AC} [3]. Presumably the undulations already present in the focal conic domains facilitate the formation of the undulations of the SD pattern.

As mentioned earlier, spherical solid particles or liquid drops of micrometric dimensions have been deposited on the central flat part of the FSF to find radial stripes in the coronal region both in the Sm*C* phase and in the Sm*A* phase above T_{AC} [12,13]. They are very similar to those found in the meniscus region of the usual FSF. The surface tension values of the deposited materials are considerably higher than that of the smectic liquid crystal, which covers the depositions, and forms a coronal meniscus region. The model proposed by us is hence applicable to these systems as well. The structure shown in Fig. 3 can be expected to be wrapped around the central particle in cylinders, the meniscus height h depending on the radial distance from the particle. In the thinner parts of the corona, far away from the deposition, the model given above can be expected to be a good approximation. Closer to the particle, as the radial distance becomes smaller, some additional curvature distortions of the **c** field arising from the cylindrical wrapping can be expected to make non-negligible contributions to the elastic energy. Further, minimization of the total energy of the entire coronal region should lead to the formation of a relatively small integral number of stripes as found in experiments. We can thus expect some quantitative changes in the calculated parameters, but the basic physical mechanism for the formation of the stripes is the same as the one discussed above.

We reemphasize that the reason for the proposed structure of Fig. 3 to be favored in the formation of SD stripes is that the only energies involved are the relatively *weak* curvature elasticities of Sm*C* LCs, without any contributions from the expensive surface energy or the compression modulus.

III. DISCUSSION AND CONCLUSIONS

As we have summarized in the Introduction, the formation of stripes along the thickness gradient of the meniscus region of FSF in Sm*C* liquid crystals has been investigated extensively. The first theoretical model [9] was based on the idea that a div**c** distortion *at the surface* could produce an electric polarization normal to the surface, which could lower the energy. The model would lead to the stripe structure even in the flat layers of the FSF, which have not been found. An experimental result to bring out the connection of stripe formation with layer height modulations was obtained using fluorescence microscopic studies [11]. Later AFM and phase shifting microscopy were used to measure the periodic surface height modulations associated with the stripes. Undulation instability of the layers in response to the reduced pressure in the meniscus region around a dispersed particle was suggested as the origin of coronal stripes [12]. The reduction in layer spacing on the transition from the Sm*A* to Sm*C* phase was suggested to give rise to the undulation instability, and the associated stripes [16], but the predicted ratio of stripe width to local thickness of the meniscus is an order of magnitude smaller than the measured values. Also, the formation of stripes in materials with a direct nematic to Sm*C* phase, and its disappearance in a material when it undergoes a transition from the Sm*C* to SmC_A phase with anticlinic tilts in neighboring layers [18] rules out this model.

Our model is based on the following arguments: (i) The meniscus surface has a *negative curvature* due to a gradient in thickness mediated by edge dislocations. A *tilting* of the molecules of the *surface layer* gives rise to a crowding of their top ends however they are aligned, costing additional energy. (ii) This energy can be lowered by changing the structure of the meniscus by exploiting the allowed k_{KC} $(\nabla \cdot \mathbf{k})(\nabla \cdot \mathbf{c})$ curvature deformation, which couples the **k** and **c** vector fields to gain energy. (iii) We have proposed a structure (Fig. 3) in which both fields vary smoothly across neighboring sections of a periodic *stripe* deformation, avoiding expensive gradients in layer spacings and walls across which the **c** field has discontinuities. (iv) The structure also does not change the area of the surfaces, or the length of the dislocation lines located at the midplane of the meniscus, avoiding additional energy costs. (v) Though the layer bending and **c**-field distortion cost energies, using reasonable values of the relevant elastic constants, our calculations show that the energy density of the structure can be lower than that of the meniscus without the formation of the stripes. (vi) The lowered energy density of the stripes is *positive*, which means that the stripes cannot form in the central region of FSFs made of flat layers. (vii) The experimentally noted linear dependence of the stripe width w and the amplitude a (which is a few % of w) on the height h of the meniscus have a natural explanation, as R_i is of molecular dimensions. (In the undulation model proposed in [16], $w \propto \sqrt{h}$). (viii) In the structure shown in Fig. 3 the relative deformation patterns at the top and bottom surfaces are shifted by $w/2$, as has been found experimentally [15]. (ix) It is clear that if successive layers have *anticlinic tilts*, the divergence of **c** will also have opposite signs in neighboring layers, and the k_{KC} term does not apply, so that the stripe structure cannot occur, as found in an experiment [18]. (x) The basic physical model can apply even above the Sm*C* to Sm*A* transition, as long as there is a reasonable tilt order in the surface region. In order to lower the energy of the bending of layers, the layer curvature and the bend angle in each section reduce, decreasing the amplitude of surface height modulation. The stripe width hardly varies with h, giving rise to straightened stripes without branching. The structure can lower energy by continuing this process, which results in a fading away of the stripes at higher temperatures. (xi) As the temperature is *lowered* towards T_{AC}, the physical processes discussed in the paper kick in, starting at the edge of the focal conics seen even in the Sm*A* phase beyond some thickness of the meniscus. Presumably the deformation already present in the focal conics facilitates the formation of SDs. (xii) The above arguments are applicable to the meniscus region generated around spherical particles deposited on the flat layers of the FSF to form coronal stripes. However, the wrapping of the structure shown in Fig. 3 in a cylindrical shell around the particle gives rise to additional curvature deformations of the **c** field, which we have not analyzed.

The proposed model thus captures the physical origin of the formation of SD patterns in the meniscus region of the Sm*C* phase and also over some temperature range above the Sm*C* to Sm*A* transition point. However, we may note that the model overestimates the amplitude of the distortion. Typically the ratio of the amplitude of SD to its width (a/w) is measured to be $\sim$1%, while the prediction made by the model is about six times larger. In one sample which has a direct transition from nematic to Sm*C* phase, the ratio appears to be far smaller, $\sim$0.01%. We can speculate about the origin of this discrepancy. As in all the earlier models, the present one also ignores the influence on the SD structure of the edge dislocation lines mediating the thickness profile of the meniscus. We argued that the length of the dislocation line, which occurs at the center of the meniscus, is unaltered by the structure shown in Fig. 3(a). However, the dislocation, which has to *bend* with the structure, has a typical line tension of $\sim 2\,10^{-3}$ N/m [2]. The bending of the line should cost a relevant curvature energy, which is reduced by pushing the dislocation line towards the surface with a lower curvature, i.e., r tends to increase from the value $(R_i + h/2)$ corresponding to the center of the meniscus. However this also *increases* the length of the dislocation, which is not favorable. The dislocation can straighten appropriately to restore the length. The net result is that the layer structure which is coupled to the shape of the dislocation line also flattens out appropriately, reducing the amplitude of the distortion. It seems that in the sample having a first order transition from the nematic to the layered Sm*C* phase directly, with a large tilt angle which is not very sensitive to variations in temperature, and forming the dislocations along with the SD structure when the FSF is drawn, this process leads to nearly flat layers. On the other hand, in systems exhibiting Sm*A* to Sm*C* transition, the tilt angle is smaller and varies with temperature, and the dislocation line can be expected to cost a lower bending energy, thus giving rise to larger a/w ratios. A detailed theoretical analysis of this process should take into account all the relevant contributions, and is beyond the scope of the present paper.

In conclusion, a few different terms of the curvature elasticity of Sm*C* liquid crystals contribute to the formation of the stripe structure in the meniscus regions of FSFs. Though the relevant elastic constants have not been measured in the experimental systems, the fact that the model can qualitatively account for all the experimental observations implies that the relative values assumed in the calculations are in the correct ballpark. It is possible that detailed experimental measurements on the stripes can lead to better estimates of the elastic constants.

ACKNOWLEDGMENT

I am thankful to the referees for asking some useful questions, and pointing out some references that were missed in the original version of the paper.

[1] P. G. de Gennes and J. Prost, *The Physics of Liquid Crystals* (Clarendon, Oxford, 1993).

[2] P. Oswald and P. Pieranski, *Smectic and Columnar Liquid Crystals* (Taylor & Francis, Boca Raton, 2006).

[3] K. Harth, B. Schulz, C. Bahr, and R. Stannarius, Soft Matter **7**, 7103 (2011).

[4] M. Selmi, J.-C. Loudet, P. V. Dolganov, T. Othman, and P. Cluzeau, Soft Matter **13**, 3649 (2017).

[5] B. Zappone *et al.*, Soft Matter **7**, 1161 (2011).

[6] K. S. Krishnamurthy, D. S. Shankar Rao, M. B. Kanakala, C. V. Yelamaggad, and N. V. Madhusudana, Phys. Rev. E **101**, 032704 (2020).

[7] R. B. Meyer, B. Stebler, and S. T. Lagerwall, Phys. Rev. Lett. **41**, 1393 (1978).

[8] K. Harth, T. Trittel, K. May, and R. Stannarius, Soft Matter **15**, 6769 (2019).

[9] R. B. Meyer and P. S. Pershan, Solid State Commun. **13**, 989 (1973).

[10] S. Dhara, R. Pratibha, and N. V. Madhusudana, Ferroelectrics **277**, 13 (2002).

[11] I. I. Smalyukh, R. Pratibha, O. D. Lavrentovich, and N. V. Madhusudana, Liq. Cryst. **30**, 877 (2003).

[12] M. Conradi, P. Ziherl, A. Sarlah, and I. Musevic, Eur. Phys. J. E **20**, 231 (2006).

[13] K. Harth and R. Stannarius, Eur. Phys. J. E **28**, 265 (2009).

[14] Ch. Bahr, C. J. Booth, D. Fliegner, and J. W. Goodby, Phys. Rev. E **52**, R4612 (1995).

[15] K. Harth, A. Eremin, and R. Stannarius, Ferroelectrics **431**, 59 (2012).

[16] J. C. Loudet, P. V. Dolganov, P. Patricio, H. Saadaoui, and P. Cluzeau, Phys. Rev. Lett. **106**, 117802 (2011).

[17] K. Harth and R. Stannarius, Ferroelectrics **468**, 92 (2014).

[18] R. Stannarius, A. Eremin, and K. Harth, Liq. Cryst. **44**, 1201 (2017).

[19] J.-C. Loudet, M. Selmi, P. V. Dolganov, T. Othman, and P. Cluzeau, Liq. Cryst. **45**, 1415 (2018).

[20] I. W. Stewart, *The Static and Dynamic Continuum Theory of Liquid Crystals* (Taylor& Francis, London, 2004).

[21] C. Zhang, A. M. Grubb, A. J. Seed, P. Sampson, A. Jakli, and O. D. Lavrentovich, Phys. Rev. Lett. **115**, 087801 (2015).